Histamine Reduces GPIbα-mediated Adhesion of Platelets to TNF-α-activated Vascular Endothelium

T. P. Brown, O. Forouzan, S. S. Shevkoplyas, and D. B. Khismatullin*

Department of Biomedical Engineering, Tulane University, New Orleans, LA, USA

* Corresponding Author. E-mail address: damir@tulane.edu

Text word count (excluding the Abstract and Reference list): 4,578

Corresponding Author:

Prof. Damir B. Khismatullin, Ph.D.
Department of Biomedical Engineering
Tulane University
Lindy Boggs Center, Suite 500
New Orleans, LA 70118
U.S.A.

Email: damir@tulane.edu
Tel.: +1-504-247-1587
Fax: +1-504-862-8779

Abstract

Histamine and tumor necrosis factor-α (TNF-α) are critical mediators of acute and chronic inflammation that are generated by mast cells and macrophages in atherosclerotic lesions or systemically during allergic attacks. Both of them induce activation of vascular endothelium and thus may play a role in thrombosis. Here we studied the interplay between histamine and TNF-α in glycoprotein (GP) Ibα-mediated platelet adhesion to cultured human vascular endothelial cells under static and shear flow conditions. The stimulation of endothelial cells with histamine or TNF-α increased the number of adherent or slow rolling GP Ibα-coated microbeads or washed human platelets. However, the application of histamine to endothelium pre-activated by TNF-α inhibited GP Ibα-mediated platelet adhesion. These effects were found to be associated with changes in the concentration of ultra large von Willebrand factor (ULVWF) strings anchored to endothelium. The results of this study indicate that histamine released during mast cell degranulation may cause or inhibit thrombosis, depending on whether it acts on resting endothelial cells or on cells pre-activated by other inflammatory stimuli.

Keywords

GP Ibα; vWF; TNF-α; histamine; platelet adhesion; endothelium

Abbreviations

GP, glycoprotein; vWF, von Willebrand factor; ULVWF, ultra large von Willebrand factor; TNF-α, tumor necrosis factor-α, ADAMTS13, a disintegrin and metalloproteinase with a thrombospondin type 1 motif - member 13; HUVEC, human umbilical vein endothelial cells; BSA, bovine serum albumin; LSGS, low serum growth supplement; EDTA, ethylenediaminetetraacetic acid; CCD, charge-coupled device.

The adhesion and accumulation of platelets at sites of vascular wall damage or inflammation is the primary event in both arterial and vein thrombosis [1-5]. It is well established [6-8] that initial adhesive interactions between platelets and vascular endothelial cells are mediated via binding of the platelet membrane glycoprotein (GP) Ib-IX-V complex to endothelial von Willebrand Factor (vWF). Endothelial cells store vWF in its highly-reactive, ultra large form (ULVWF) within Weibel-Palade bodies [9-11] from which it is secreted constitutively or in response to thrombogenic stimuli [12-14]. A portion of secreted ULVWF strings are anchored to the endothelial cell membrane [15, 16]. Platelets adhere to these strings because of high-affinity binding between the vWF A1 domain and the GP Ibα subunit of the GP Ib-IX-V complex [17, 18]. This process is, however, tightly regulated by hemostatic mediators such as the plasma protease ADAMTS-13, which promptly cleaves ULVWF into smaller, less reactive dimers, thus preventing the formation of occlusive thrombi [19-21].

Tumor necrosis factor-α (TNF-α) and histamine are important mediators of chronic and acute inflammation. TNF-α produced by tissue resident macrophages activate endothelial cells [22] and thus increases the flux of leukocytes to the inflamed tissue [23]. Histamine causes inflammation when it is released from mast cells and basophils in response to allergen [24-26]. It can also be secreted by activated platelets [27, 28]. Bernardo et al. [14] demonstrated that TNF-α stimulates ULVWF secretion and platelet aggregation to ULVWF strings. Numerous evidence indicates that histamine can induce the secretion of proteins from Weibel-Palade bodies, including P-selectin and ULVWF [2, 29-32]. Interestingly, ULVWF generated through endothelium activation by histamine alone remains associated with the endothelial cell membrane, likely due to the involvement of P-selectin in the ULVWF anchorage [16]. This leads to rapid accumulation of platelets at histamine-activated endothelium [16, 27, 33].

Both TNF-α and histamine can simultaneously reach a high concentration in specific regions of the body. For instance, the histamine level is high during allergic attacks [24], and patients with allergy may have chronic inflammatory conditions such as atherosclerosis at which TNF-α is extensively released [34]. Histamine secretion from mast cells abundantly found in the atherosclerotic plaques [35] contributes to atherosclerosis even in the absence of the allergic response [36, 37]. Meanwhile, platelets play a crucial role in this pathological process by either recruiting leukocytes [38, 39] or by causing acute thrombotic events after rupture of a vulnerable plaque [40]. The interplay between TNF-α and histamine in platelet-endothelium adhesion and thrombus formation is not yet studied. Here, we investigate adhesive interactions of GP Ibα-coated microbeads and human platelets with cultured human endothelial cells exposed to both TNF-α and histamine under static and shear flow conditions.

Materials and Methods

Reagents

Histamine, TNF-α, bovine serum albumin (BSA), 2-(N-morpholino)ethanesulfonic (MES) acid hydrate, and 2% gelatin were obtained from Sigma-Aldrich (St. Louis, MO). Human recombinant glycoprotein Ibα (GP Ibα) was purchased from R&D systems (Minneapolis, MN). 2.0 μm diameter carboxylate-modified fluorescent latex microspheres (505/515 nm, FluoSpheres®) and 1-ethyl-3-(3-dimethylaminopropyl) carbodiimide (EDAC) were purchased from Invitrogen (Carlsbad, CA). GTI-V3P monoclonal mouse anti-human-vWF (GTI Diagnostics, Waukesha, WI) was used to block the A1 domain of vWF.

Endothelial culture

Primary human umbilical vein endothelial cells (HUVEC) were purchased from Invitrogen. Endothelial cells were grown out in T-75 flasks in low serum growth medium (M200-LSGS; Invitrogen) supplemented with antibiotics. When 80% or greater confluence was reached, the cells were harvested by treatment with 0.1% trypsin in EDTA (Sigma-Aldrich), yielding approximately 2.0×10^6 cells per flask. HUVEC were reseeded, at passage 4-6, in 0.1% gelatin-coated 24-well plates for static adhesion assays. Experiments were conducted within 24 hours after HUVEC reached more than 90% confluence in the 24-well plates. All the cells were maintained at 37°C in a 5% CO_2 humidified incubator.

Preparation of GP Ibα-coated microbeads

Covalent coupling of the amino-terminal end of GP Ibα to the carboxylate group on the surface of latex microspheres (microbeads) was accomplished through carbodiimide chemistry, catalyzed by EDAC [41], using the protocol by Liu *et al.* [42]. Briefly, 400 μL of MES buffer

was added to a 100 µL aliquot of microbeads and mixed by aspiration and sonication for five minutes. The resulting suspension was then centrifuged at 6,708×g for 10 minutes. Following centrifugation, the microbead pellet was isolated and re-suspended in 500 µL of MES buffer. This wash procedure was repeated three times, with the microbead pellet re-suspended in 100 µL of MES in the final stage. 20 µL of EDAC was then added and mixed by aspiration, followed by sonication. After a 20 minute incubation period with EDAC at room temperature, 2.5 µL of recombinant human GP Ibα (50 µg/mL), calculated to yield the surface density of 300 sites/µm^2, was added to the microbead-EDAC suspension. The final suspension was incubated at room temperature for at least 12 hours before an adhesion assay, with continuous gentle vortexing.

Following the covalent attachment of GP Ibα to the microbead surface, the microbeads were re-suspended in 400 µL of phosphate-buffered saline (PBS), sonicated to break apart any clumps that may have formed during the incubation period, and subsequently separated by centrifugation at 6,708×g for 10 minutes. After two additional wash steps conducted in 500 µL PBS, protein-coated microbeads were re-suspended in 3 mL of 1.5% BSA, which served to block non-specific binding, finally yielding a concentration of 400,000 particles/µL.

The control group of microbeads was washed as described above. However, following the third wash step the microbeads were re-suspended in 2% BSA and incubated overnight with gentle vortexing. The suspension of control microbeads were washed twice in PBS and re-suspended in 1.5% BSA immediately before an adhesion assay was performed.

Preparation of human platelets

Human venous blood was collected from healthy consenting volunteers into 4 mL Vacutainer tubes (K_2EDTA, BD, Franklin Lakes, NJ) and used within 4 hours of donation. Platelet rich plasma was prepared by centrifugation of whole blood samples (400×g, 4 min).

Whole blood and platelet rich plasma were analyzed for platelet and red blood cell content using a hemocytometer (BD, Franklin Lakes, NJ). Platelet rich plasma was then diluted with PBS to the desired platelet concentration, and then used immediately in the adhesion experiments.

Cell-free model to study GP Ibα-mediated platelet adhesion

We developed a well-controlled system consisting of carboxylate-modified fluorescent microbeads to quantitatively describe GP Ibα-mediated platelet adhesion to stimulated endothelial cells. The microbead diameter (2.0 μm) was selected based on measured diameters of human and mouse platelets (0.5 to 3.0 μm [43, 44]). Each platelet has 15,000 to 25,000 copies of GP Ibα [45, 46]. Based on this estimation and using the literature value of 50 μm^2 [47] for the surface area of a washed human platelet, the lower bound for the GP Ibα density is about 300 sites/μm^2. Assuming spherical geometry, our microbeads were coated with GP Ibα at this value of the receptor density. It is anticipated that a higher density of GP Ibα will make the effects we observed more pronounced. The concentration of microbeads in the BSA solution (400,000 particles /μL) was carefully controlled in adhesion assays to mimic platelet-endothelial interactions in vivo. The range of platelet concentrations in human blood is between 150,000 and 450,000 platelets/μL [48].

Static Adhesion Experiments

Confluent groups of HUVEC in a 24-well tissue culture plate were left untreated (control) or incubated with TNF-α (50 ng/mL), histamine (10^{-6} mol/L), or their combination for one hour at 37ºC. In the combined activation group, histamine was introduced into the growth medium 30 minutes into the TNF-α activation period. The supernatant from each well was then removed and GP Ibα-coated microbeads were applied to HUVEC for five minutes. All wells

were then washed three times with PBS to remove any microbeads that had not firmly attached to the endothelium. After the wash procedure had ended, the wells were imaged under an inverted microscope (Nikon Eclipse TiS) using 40X objective. Four randomly selected images from each well were captured with a CCD camera (QImaging Retiga EXi), and saved in the TIFF format at a resolution of 1392×1040 pixels.

Anti-body blocking experiments were also conducted to evaluate the influence of GP Ibα-vWF binding under the inflammatory conditions studied. The vWF blocking assay was identical to the static adhesion assay with the exception that the cells in the blocking antibody groups were incubated with 6.7 µL of V3P in 200 µL of 2% BSA in PBS for 30 minutes at 37ºC immediately following TNF-α and/or histamine incubation, while other groups received just 2% BSA in PBS. GP Ibα-coated microbeads were then applied and imaged as described above.

Static adhesion of washed human platelets to histamine-activated endothelium was also analyzed to validate the cell-free platelet model. In this experiment, HUVEC were stimulated with 0, 10^{-4}, or 10^{-6} mol/L of histamine for five minutes before applying GP Ibα-coated microbeads and/or platelets. The platelet and microbead adhesion to HUVEC was quantified through image analysis using a custom MATLAB script (**Fig. 2)**. It should be noted that the systematic histamine concentration in blood can increase to 10^{-7} mol/L during allergic attack [49]. The local concentration of serum histamine several minutes to hours after allergen exposure may far exceed its measured systematic value. Spikes in the histamine concentration to much higher than 10^{-7} mol/L may occur locally in the tissue containing a large number of activated mast cells. To model this situation, we considered the histamine concentration of 10^{-6} mol/L in the majority of experiments. 10^{-4} mol/L histamine was used only for short-term (5 minutes) activation of HUVEC for the model validation purpose. It should be noted that histamine with

this concentration was used in numerous in vitro experiments [50-54]. 10^{-4} mol/L is a threshold concentration for the histamine effect on leukocyte rolling [29]. This level is shown to saturate the vWF response [16, 30].

Flow Chamber Experiments

GP Ibα-coated microbeads were perfused over confluent HUVEC monolayers cultured in a commercially available microfluidic flow chamber (Bioflux 200, Fluxion Biosciences, San Francisco, CA). Briefly, passage 3-5 HUVEC were seeded in gelatin-coated micro-channels of a 48-well Bioflux plate at a density of $5x10^6$ cells/mL. The width and height of these micro-channels were 350 and 70 μm, respectively. Media changes were performed twice daily for 2-3 days until confluence was reached. Confluent HUVEC monolayer in micro-channels were left untreated (control) or exposed to selected inflammatory mediators (50 ng/mL of TNF-α, 10^{-6} mol/L of histamine, or their combination) for one hour. Following the activation period, HUVEC-lined micro-channels were washed by perfusion with the growth medium (M200). Fluorescent GP Ibα-coated microbeads were then perfused over each micro-channel for a period of 2 minutes under physiologic shear flow conditions (wall shear stress of 0.6 dyn/cm^2, wall shear rate of ~70 s^{-1}). Fluorescent images of the flowing beads were visualized using a 10X objective in an inverted microscope (Nicon Eclipse TiS), and a total of 2400 images per micro-channel were captured by a digital CCD camera (Qimaging Retiga EXi) at 20 frames/s. The number of microbeads slowly rolling along the stimulated endothelium was quantified frame-by-frame using methods similar to the analysis of static adhesion (see below) and normalized to the control.

Quantification of Microbead and Platelet Adhesion

Digital images were analyzed using a custom program written in MATLAB® (Mathworks, Natick, MA). Briefly, the original image **(Fig. 1A)** was imported into MATLAB® as an array of intensity values. The image contrast was increased and further adjusted by the Contrast Limited Adaptive Histogram Equalization (CLAHE) technique using the image processing toolbox of MATLAB **(Fig. 1B).** Following contrast standardization, the grayscale image was converted into a binary, black and white image. The edges of the objects (including beads, cells, and debris) in this image were then detected using an edge-detection algorithm with a Sobel filter **(Fig. 1C)**. The image was then dilated, the holes within closed borders were filled in, and any objects contacting the border of the image were removed. The filled image with clear borders then underwent a two-stage erosion algorithm, which isolated partially connected and small objects within the image. The debris field resulting from the erosion step consisted of small amorphous objects representing cellular fragments **(Fig. 1D)**, which were then removed from the image through a morphological opening algorithm **(Fig. 1E)**. Any remaining small objects were finally removed using a filter targeting objects with an area less than 110 pixels, or 60% of the calculated average microbead area. The perimeter of the remaining objects in the resulting black and white image outlining only the microbeads of interest was determined. The original image was then overlaid with the enhanced green-colored borders of the microbeads **(Fig. 1F).**

Morphologically opened images (**Fig. 1D**) depict adherent microbeads, i.e., the microbeads left after the wash procedure, as white 'blobs' completely surrounded by the black background. Since closely associated microbeads may be counted as one object by this method, we first determined the average pixel-area of a microbead within the sequence of 36 to 48 images. 12 microbeads were selected from the images and their area was averaged, yielding the

value of 205 pixels per microbead. The number of microbeads within each blob was then calculated by dividing the area of the blob by the pre-determined single microbead area. This number was summed over all blobs to determine the total number of adherent microbeads in the image.

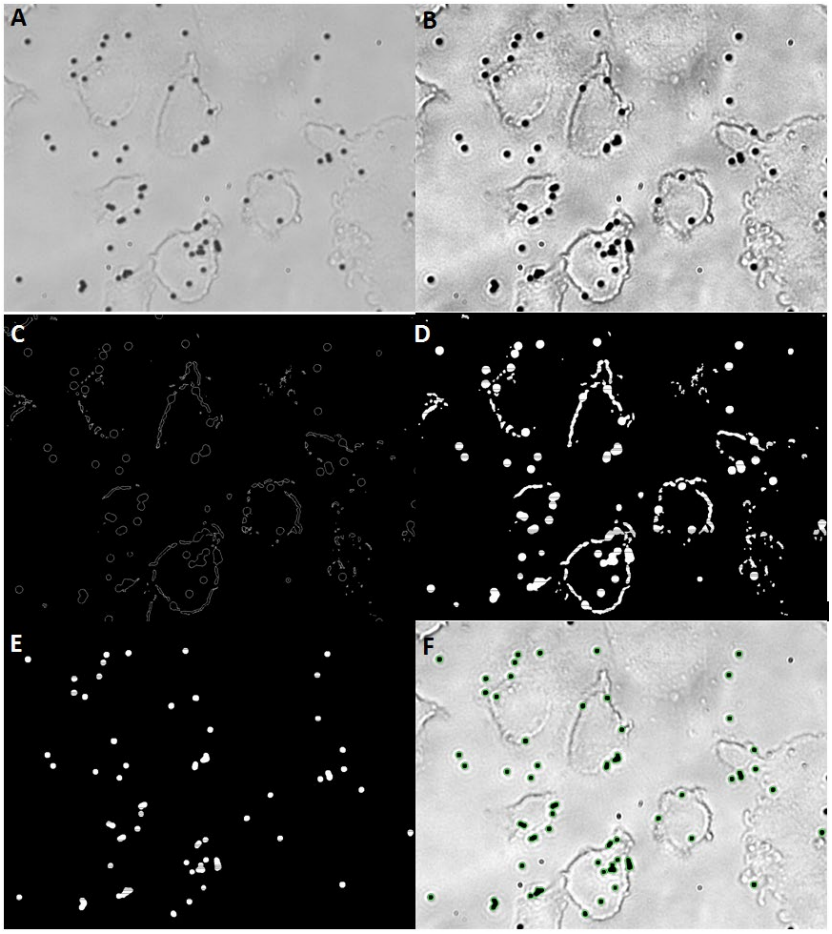

Figure 1: *Digital image analysis technique used to quantify adhesion of microbeads and platelets to HUVEC.* ***(A)*** *Original image.* ***(B)*** *Image following contrast enhancement to facilitate detection of the edges of microbeads or platelets (point to black spots).* ***(C)*** *Dark objects were outlined based on their grayscale intensity relative to the background.* ***(D)*** *These borders were used to generate a binary image with filled areas between closed borders.* ***(E)*** *Cellular debris and other unwanted objects in the closed-border image were removed through morphological opening algorithm, followed by a dilation filter to remove small objects, producing a binary representation of adherent microbeads/platelets.* ***(F)*** *This binary image was used to generate borders of microbeads/platelets which were then overlaid onto the original image for visualization.*

Statistical Analysis

In static adhesion experiments, the data from four images per well were averaged together for three wells examined per experimental group. For flow experiments, the number of slow rolling microbeads was calculated on a frame by frame basis, which was then averaged across the entire image sequence. Reported is the mean flux of rolling microbeads averaged across each individual microchannel, generating five individual data points from 12000 images that were analyzed. All independent experiments were done in triplicate. Results are presented as the mean ± standard error of the mean (SEM). Statistical analysis was evaluated using a two-tailed, unpaired Student's t-test. P-values less than 0.05 were considered statistically significant.

Results

Cell-Free Platelet Model Validation

GP Ibα-coatedmicrobeads were evaluated against BSA-coated microbeads to assess non-specific interactions to the tissue culture plate, gelatin coating, resting endothelium, and histamine-stimulated endothelium. Both BSA and GP Ibα-coated microbeads were applied to gelatin-coated tissue culture plates in order to demonstrate the latex microbead interactions are HUVEC-dependent **(Fig. 2A)**. The specificity of GP Ibα-coated microbeads for the HUVEC monolayer was then evaluated on both resting HUVEC and HUVEC stimulated with 10^{-4} M histamine in M200 for 5 minutes **(Fig. 2B)**.

Figure 3A shows that GP Ibα-coated microbeads (small bright circles) were minimally adherent to the resting HUVEC monolayer. Following stimulation with 10^{-4} mol/L of histamine, secreting ULVWF on HUVEC promoted increased microbead adhesion, and endothelial cells retracted pseudopods and became round in shape with more gaps between cells (**Fig. 3B**). Only a

few human platelets (white amorphous dots) were seen attached to the resting endothelium (**Fig. 3C**). As in studies using microbeads, stimulation with 10^{-4} mol/L of histamine has been observed to induce endothelial secretion of ULVWF which occurred primarily in a basolateral direction and created gaps in the previously confluent monolayer **(Fig. 3D)**. Thus, both platelets and GP Ibα-coated microbeads adhered primarily around the periphery of stimulated HUVEC, which is consistent with the localized presence of ULVWF in this region.

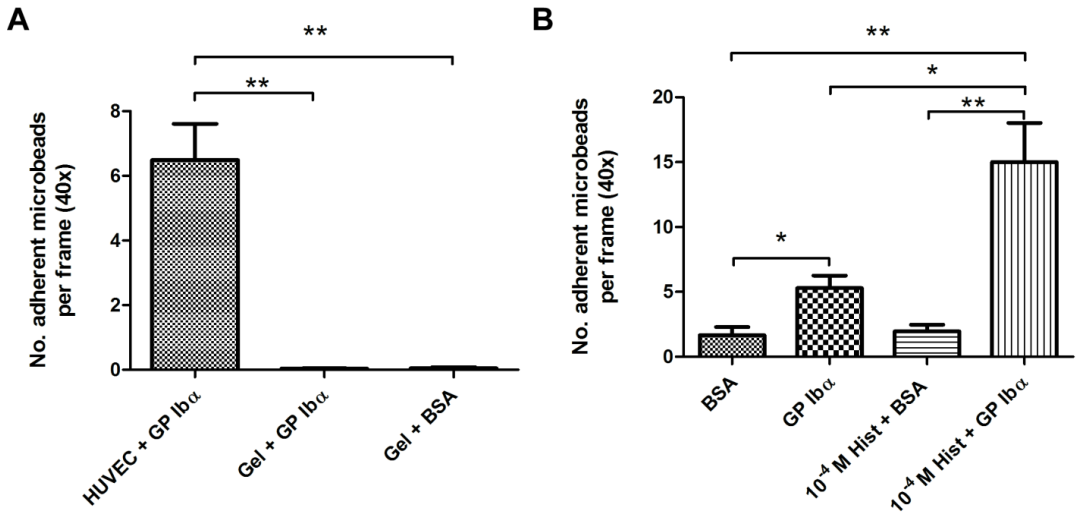

Figure 2: *Specificity of GP Ibα-coated microbead adhesion to HUVEC. (A) Neither GP Ibα- nor BSA-coated microbeads adhered in any significant manner to the 0.1% gelatin-in-PBS (gel) substrate, however, GP Ibα-mediated adhesion increased significantly from 0.0355 ± 0.0175 beads per frame (BPF) on gelatin to 6.49 ± 1.12 BPF on HUVEC.* ***(B)*** *GP Ibα-coated microbeads adhere significantly stronger to HUVEC monolayer than do BSA-coated microbeads: 5.29 ± 0.966 GP Ibα-coated microbeads were bound per frame on resting HUVEC, compared to 1.67 ± 0.631 BSA-coated microbeads. Histamine had no significant effect on BSA adhesion (1.67 ± 0.631 vs 1.96 ± 0.522). However, GP Ibα adherence was significantly greater to histamine-stimulated HUVEC (15.0 ± 3.03 BPF) compared to resting HUVEC (5.29 ± 0.966 BPF). Shown are Mean ± SEM of six independent data points. * $p < 0.05$, ** $p < 0.01$.*

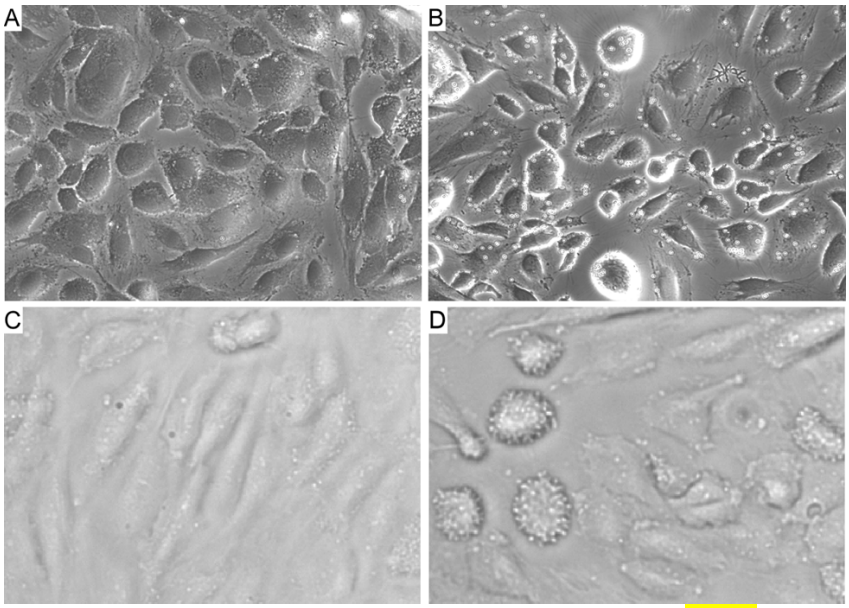

Figure 3*: Phase-constrast images showing adhesion of microbeads* ***(A,B)*** *and platelets* ***(C,D)*** *to resting and stimulated HUVEC.* ***(A)*** *GP Ibα-coated microbeads (small bright circles) were minimally adherent to a resting HUVEC monolayer.* ***(B)*** *Following stimulation with 10^{-4} mol/L of histamine, endothelial cells retract pseudopods and become round in shape, forming gaps in the previously confluent monolayer. Adherent GP Ibα-coated microbeads are found around the periphery of histamine-activated endothelial cells due to the localized presence of ULVWF strings in this region.* ***(C)*** *Human platelets (tiny white specs against grey background and cells) adhere minimally to a resting HUVEC monolayer.* ***(D)*** *HUVEC stimulation with 10^{-4} mol/L of histamine significantly increases platelet adhesion to HUVEC borders.*

Figure 4 demonstrates that both platelets and GP Ibα-coated microbeads adhere to histamine-stimulated endothelium in a dose-dependent fashion. As seen in **Fig. 4A**, stimulation with 10^{-4} mol/L of histamine significantly ($p < 0.0001$) increased the number of adherent microbeads to 4.49 ± 0.600 times that of the control. Similarly, the number of adherent platelets significantly ($p < 0.05$) increased to 3.16 ± 0.745 of the control value following stimulation with the same dose of histamine. **Figure 4B** depicts the data shown in **Fig. 4A** with normalized adherence of GP Ibα-coated microbeads plotted against the normalized adhesion of washed human platelets. A linear regression gave us the equation of the best-fit line for our data (**Fig.**

4B), yielding an r^2 value of 0.999. This indicates that there exists a strong correlation between GP Ibα-coated microbead and platelet adhesion to activated endothelium.

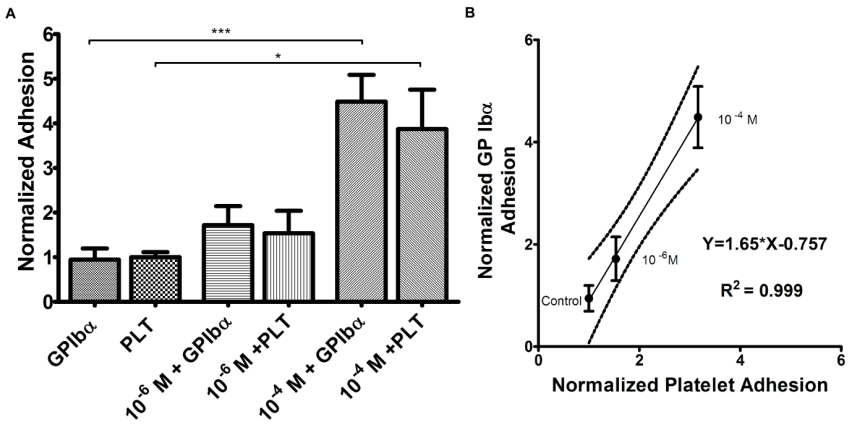

Figure 4: *Correlation in microbead and platelet adhesion to stimulated HUVEC under static conditions* ***(A)*** *Both human platelets (PLT) and GPIbα-coated microbeads adhere to histamine-stimulated endothelium in a concentration dependent manner. Here, 10^{-4} M and 10^{-6} M indicate HUVEC incubation with 10^{-4} mol/L and 10^{-6} mol/L of histamine, respectively.* ***(B)*** *The correlation curve constructed from the GPIbα and PLT data in (A). Dotted lines show the 95% confidence interval. The correlation coefficient $r^2 = 0.999$. Mean ± SEM of nine independent data points, normalized to GPIbα-coated microbead control with basis 1 * $p < 0.05$, *** $p < 0.0001$.*

Combined effect of TNF-α and histamine

As in the case of HUVEC exposed to histamine alone (**Fig. 4A**), the one hour incubation of HUVEC with 50 ng/mL of TNF-α significantly increased the number of adherent GP Ibα-coated microbeads (2.47 ± 0.392 of the control value, $p < 0.05$) (**Fig. 5A**). However, when TNF-α was co-incubated with 10^{-6} mol/L of histamine, a significant decrease ($p < 0.05$, 52.7%) in microbead adhesion was observed, when compared to the TNF-α alone activation. As seen in **Fig. 5A**, the number of microbeads adherent to TNF-α + histamine-activated endothelium was just 1.17 ± 0.187 of the control value. **Figure 5B** shows that the observed effects of TNF-α and histamine can be blocked by HUVEC incubation with a monoclonal antibody VP3 directed against the A1 domain of vWF. Specifically, adding this antibody to resting, TNF-α-activated,

and TNF-α + histamine-activated endothelium reduced the number of adherent microbeads to 0.714 ± 0.0714, 0.929 ± 0.228, and 0.696 ± 0.142 of the control value, respectively. Thus, both TNF-α effect and the decrease in the number of adherent microbeads with histamine stimulation of TNF-α-activated endothelium are associated with changes in the concentration of ULVWF strings anchored to endothelium.

The GP Ibα-coated microbead adhesion to HUVEC exposed to single and multiple inflammatory mediators was quantified under flowing conditions (**Fig. 6**). HUVEC monolayers stimulated with 10^{-6} mol/L of histamine demonstrated a slight, but not significant, increase in the number of slow rolling microbeads (measured as beads per frame (BPF) normalized against the control) than did the unstimulated HUVEC monolayer (1.25 ± 0.181 vs. 1.00 ± 0.0944, i.e., 25% increase). Stimulation with 50 ng/mL of TNF-α produced a significantly ($p < 0.05$) greater effect on GP Ibα-mediated adhesion, resulting in a 33% increase in the number of slow rolling microbeads compared to the control (1.33 ± 0.0916). As in static adhesion experiments, the number of microbeads interacting with TNF-α-activated HUVEC under flow was significantly ($p < 0.05$) lower when HUVEC was additionally stimulated with histamine (1.01 ± 0.041 vs. 1.33 ± 0.0916). It is worth mentioning that GP Ibα-coated microbeads were observed to adhere to the periphery of the endothelial cells under flow conditions, which is slightly different from the behavior of platelets that adhere like "beads on a string" [19]. This discrepancy may be attributed to the lack of secondary adhesion receptors such as GPIIb/IIIa ($\alpha_{IIb}\beta_3$), which would form stronger bonds with vWF than GP Ibα.

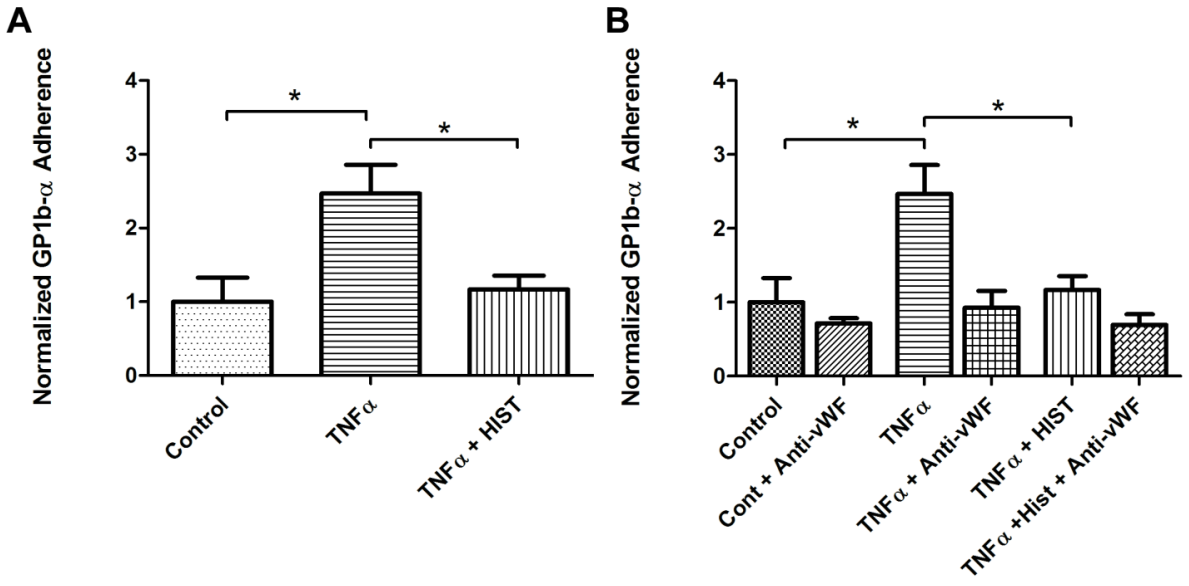

Figure 5: *Effect of TNF-α and histamine on adhesion of GP Ibα-coated microbeads (GP1b-α) to HUVEC under static conditions.* ***(A)*** *HUVEC exposure to TNF-α at 50 ng/mL for 60 minutes significantly increases microbead adhesion to HUVEC. When 10^{-6} mol/L of histamine (HIST) was added alongside TNF-α, a significant decrease in microbead adhesion was observed.* ***(B)*** *For each inflammatory regime tested in (A)****,*** *the same experiment was performed in the presence of a monoclonal antibody VP3 directed against the vWF A1 domain. A 30 minute incubation period with VP3 resulted in reduced microbead adhesion to near control values. Mean ± SEM of nine independent data points, normalized to control with basis 1. * $p < 0.05$.*

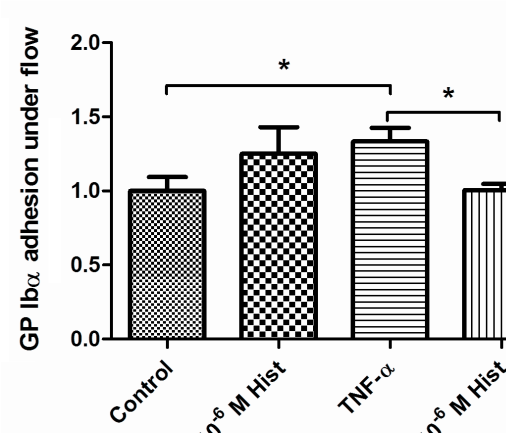

Figure 6: *Effect of TNF-α and histamine (Hist) on adhesion of GP Ibα-coated microbeads to HUVEC under flow conditions. The number of slow rolling microbeads increases with HUVEC exposure to 10^{-6} mol/L of histamine or 50 ng/mL of TNF-α. The combined exposure of HUVEC to TNF-α and histamine, however, results in a significant decrease in rolling adhesion of microbeads, compared to TNF-α alone stimulation. Mean ± SEM of six independent data points, normalized to control with basis 1. * $p < 0.05$.*

Discussion

The results presented in this report suggest that histamine may play a dual role in platelet adhesion to vascular endothelium. When applied to resting endothelial cells, histamine increases the number of ULVWF strings on the endothelial surface and thus induces platelet accumulation on endothelial cells, in line with published data [16]. However, if histamine is released near endothelium activated by inflammatory mediators such as TNF-α, it may have an inhibitory role in GP Ibα-mediated platelet-endothelial cell interactions. This is most likely caused by the histamine-induced detachment of endothelium-anchored ULVWF strings secreted after TNF-α exposure. This detachment may occur, for example, due to histamine-induced F-actin redistribution in endothelial cells with disappearance of dense peripheral bands of F-actin and stress fibers [55, 56]. The weakening and rearrangement of the actin cytoskeleton induced by histamine may reduce the strength of ULVWF binding to the endothelial cell surface [57]. The dual, paradoxical effect of histamine on platelet-endothelium adhesion may be one of the reasons behind conflicting reports on the role of mast cells in thrombosis. Mast cell-deficient mice were found to be more susceptible to lethal thromboembolism than wild-type mice, and evidence shows that mast cells accumulate at sites of venous thrombosis, where they serve as repair cells [58, 59]. On the other hand, mast cells activated by diesel exhaust particles were found to initiate inflammation and thrombosis in the lungs of hamsters [60]. Thus, histamine released from mast cells may cause or inhibit thrombosis, depending on whether it acts on resting endothelial cells or on cells pre-activated by other inflammatory stimuli.

A large number of mast cells are colocalized with macrophages in atherosclerotic plaques [35], where their activation leads to a significant increase in local histamine concentration [36, 37, 61]. Our data underlines the need for understanding whether mast cells are already present at sites where atherosclerosis would be developed or they migrate to early atherosclerotic lesions in

response to stimuli released by activated cells in these regions. In the former case, platelet adhesion to histamine-activated arterial endothelium could initiate atherosclerosis. Indeed, adherent platelets can capture flowing monocytes via platelet P-selectin binding to monocyte PSGL-1 [41, 62]. This leads to the accumulation of monocytes in the intimal layer of an artery, where monocytes differentiate into macrophages and then foam cells. If the latter case is true, histamine release from mast cells will have an anti-thrombotic effect on dysfunctional endothelium at the plaque. However, activated mast cells will still cause monocyte adhesion and transendothelial migration. Indeed, our recent investigation [63] shows that the number of slow rolling and firmly adherent monocytes is higher on endothelium activated sequentially by TNF-α and histamine than that on endothelium activated by TNF-α alone, with no slow rolling or firm adhesion events observed when endothelial cells are exposed to histamine alone. This synergestic effect indicates that histamine release from mast cell may lead to direct capture of monocytes by endothelium (i.e., without involvement of platelets) provided endothelium is pre-activated by TNF-α.

The methods used in this work are well suited to study functional characteristics of receptor-ligand interactions involved in thrombosis. Fluorescent latex microbeads can be covalently coated with platelet, leukocyte, or any other recombinant protein at physiologically relevant concentrations, forming a model ideal for studying adhesion, translocation, and aggregation under well controlled conditions free from the involvement of other proteins, cytokines, and cellular elements present in previous studies using viable platelets or CHO cells [16, 62]. Furthermore, the difficulty in working with human platelets has impeded their use in quantitative studies. Platelets become activated extremely easily, for instance, centrifuging platelets in PBS yields a platelet pellet which cannot be broken apart and re-suspended. For these

reasons, we propose the use of GP Ibα-coated microbeads as a model to evaluate platelet adhesion to the vascular endothelium, the first step in thrombosis and related pathologies.

In summary, we developed a cell-free model of a human platelet by covalently coating latex microbeads with human recombinant GP Ibα. Using this model, we were able to quantify GP Ibα-mediated platelet adhesion to histamine- and/or TNF-α-activated endothelium under static and flow conditions. The results of this work demonstrate that histamine may have both stimulatory and inhibitory effects on platelet-endothelial adhesion: resting endothelium exposed to histamine is more adhesive to platelets, while histamine exposure of TNF-α-activated endothelium leads to reduced adhesion of platelets. Future studies will specifically examine the role of mast cell activation in platelet-endothelial cell interactions.

Conflict of Interest Statement

The authors declare that they have no conflict of interest.

Acknowledgements

This work was supported by Louisiana Board of Regents grant LEQSF(2011-14)-RD-A-24 to D.B.K. We thank Michael Moore for helpful discussions and Chong Chen for the help in cell culture.

References

[1] Austin SK. Haemostasis. Medicine. 2009;37:133-6.

[2] Andre P, Denis CV, Ware J, Saffaripour S, Hynes RO, Ruggeri ZM, et al. Platelets adhere to and translocate on von Willebrand factor presented by endothelium in stimulated veins. Blood. 2000;96:3322-8.

[3] Nieswandt B, Pleines I, Bender M. Platelet adhesion and activation mechanisms in arterial thrombosis and ischaemic stroke. J Thromb Haemost. 2011;9 Suppl 1:92-104.

[4] Brill A, Fuchs TA, Chauhan AK, Yang JJ, De Meyer SF, Kollnberger M, et al. von Willebrand factor-mediated platelet adhesion is critical for deep vein thrombosis in mouse models. Blood. 2011;117:1400-7.

[5] Takahashi M, Yamashita A, Moriguchi-Goto S, Marutsuka K, Sato Y, Yamamoto H, et al. Critical role of von Willebrand factor and platelet interaction in venous thromboembolism. Histol Histopathol. 2009;24:1391-8.

[6] Fredrickson BJ, Dong JF, McIntire LV, Lopez JA. Shear-dependent rolling on von Willebrand factor of mammalian cells expressing the platelet glycoprotein Ib-IX-V complex. Blood. 1998;92:3684-93.

[7] Bonnefoy A, Vermylen J, Hoylaerts MF. Inhibition of von Willebrand factor-GPIb/IX/V interactions as a strategy to prevent arterial thrombosis. Expert Rev Cardiovasc Ther. 2003;1:257-69.

[8] Sugimoto M, Miyata S. Functional property of von Willebrand factor under flowing blood. Int J Hematol. 2002;75:19-24.

[9] Wagner DD, Bonfanti R. von Willebrand factor and the endothelium. Mayo Clin Proc. 1991;66:621-7.

[10] Ruggeri ZM. Structure of von Willebrand factor and its function in platelet adhesion and thrombus formation. Best Pract Res Clin Haematol. 2001;14:257-79.

[11] Rondaij MG, Bierings R, Kragt A, van Mourik JA, Voorberg J. Dynamics and plasticity of Weibel-Palade bodies in endothelial cells. Arterioscler Thromb Vasc Biol. 2006;26:1002-7.

[12] Sadler JE. Biochemistry and genetics of von Willebrand factor. Annu Rev Biochem. 1998;67:395-424.

[13] Vischer UM, Ingerslev J, Wollheim CB, Mestries JC, Tsakiris DA, Haefeli WE, et al. Acute von Willebrand factor secretion from the endothelium in vivo: assessment through plasma propeptide (vWf:AgII) Levels. Thromb Haemost. 1997;77:387-93.

[14] Bernardo A, Ball C, Nolasco L, Moake JF, Dong JF. Effects of inflammatory cytokines on the release and cleavage of the endothelial cell-derived ultralarge von Willebrand factor multimers under flow. Blood. 2004;104:100-6.

[15] Chauhan AK, Goerge T, Schneider SW, Wagner DD. Formation of platelet strings and microthrombi in the presence of ADAMTS-13 inhibitor does not require P-selectin or beta3 integrin. J Thromb Haemost. 2007;5:583-9.

[16] Padilla A, Moake JL, Bernardo A, Ball C, Wang Y, Arya M, et al. P-selectin anchors newly released ultralarge von Willebrand factor multimers to the endothelial cell surface. Blood. 2004;103:2150-6.

[17] Miura S, Li CQ, Cao Z, Wang H, Wardell MR, Sadler JE. Interaction of von Willebrand factor domain A1 with platelet glycoprotein Ibalpha-(1-289). Slow intrinsic binding kinetics mediate rapid platelet adhesion. J Biol Chem. 2000;275:7539-46.

[18] Doggett TA, Girdhar G, Lawshe A, Schmidtke DW, Laurenzi IJ, Diamond SL, et al. Selectin-like kinetics and biomechanics promote rapid platelet adhesion in flow: the GPIb(alpha)-vWF tether bond. Biophys J. 2002;83:194-205.

[19] Dong JF, Moake JL, Nolasco L, Bernardo A, Arceneaux W, Shrimpton CN, et al. ADAMTS-13 rapidly cleaves newly secreted ultralarge von Willebrand factor multimers on the endothelial surface under flowing conditions. Blood. 2002;100:4033-9.

[20] Turner NA, Nolasco L, Ruggeri ZM, Moake JL. Endothelial cell ADAMTS-13 and VWF: production, release, and VWF string cleavage. Blood. 2009;114:5102-11.

[21] Zhang X, Halvorsen K, Zhang CZ, Wong WP, Springer TA. Mechanoenzymatic cleavage of the ultralarge vascular protein von Willebrand factor. Science. 2009;324:1330-4.

[22] Zhang H, Park Y, Wu J, Chen X, Lee S, Yang J, et al. Role of TNF-alpha in vascular dysfunction. Clin Sci (Lond). 2009;116:219-30.

[23] Ley K. Molecular mechanisms of leukocyte recruitment in the inflammatory process. Cardiovasc Res. 1996;32:733-42.

[24] Akdis CA, Blaser K. Histamine in the immune regulation of allergic inflammation. J Allergy Clin Immunol. 2003;112:15-22.

[25] Proud D, Bailey GS, Naclerio RM, Reynolds CJ, Cruz AA, Eggleston PA, et al. Tryptase and histamine as markers to evaluate mast cell activation during the responses to nasal challenge with allergen, cold, dry air, and hyperosmolar solutions. J Allergy Clin Immunol. 1992;89:1098-110.

[26] Beauvais F, Bidet B, Descours B, Hieblot C, Burtin C, Benveniste J. Regulation of human basophil activation. I. Dissociation of cationic dye binding from histamine release in activated human basophils. J Allergy Clin Immunol. 1991;87:1020-8.

[27] Masini E, Di Bello MG, Raspanti S, Fomusi Ndisang J, Baronti R, Cappugi P, et al. The role of histamine in platelet aggregation by physiological and immunological stimuli. Inflamm Res. 1998;47:211-20.

[28] Nakahodo K, Saitoh S, Nakamura M, Kosugi T. Histamine release from rabbit platelets by platelet-activating factor (PAF). Arerugi. 1994;43:501-10.

[29] Kubes P, Kanwar S. Histamine induces leukocyte rolling in post-capillary venules. A P-selectin-mediated event. J Immunol. 1994;152:3570-7.

[30] Hattori R, Hamilton KK, Fugate RD, McEver RP, Sims PJ. Stimulated secretion of endothelial von Willebrand factor is accompanied by rapid redistribution to the cell surface of the intracellular granule membrane protein GMP-140. J Biol Chem. 1989;264:7768-71.

[31] Nolasco LH, Turner NA, Bernardo A, Tao Z, Cleary TG, Dong J-f, et al. Hemolytic uremic syndrome–associated Shiga toxins promote endothelial-cell secretion and impair ADAMTS13 cleavage of unusually large von Willebrand factor multimers. Blood. 2005;106:4199-209.

[32] Esposito B, Gambara G, Lewis AM, Palombi F, D'Alessio A, Taylor LX, et al. NAADP links histamine H1 receptors to secretion of von Willebrand factor in human endothelial cells. Blood. 2011;117:4968-77.

[33] López JA, Dong J-f. Cleavage of von Willebrand factor by ADAMTS-13 on endothelial cells. Seminars in Hematology. 2004;41:15-23.

[34] Jovinge S, Ares MP, Kallin B, Nilsson J. Human monocytes/macrophages release TNF-alpha in response to Ox-LDL. Arterioscler Thromb Vasc Biol. 1996;16:1573-9.

[35] Jeziorska M, McCollum C, Woolley DE. Mast cell distribution, activation, and phenotype in atherosclerotic lesions of human carotid arteries. J Pathol. 1997;182:115-22.

[36] Kovanen PT. Mast cells in atherogenesis: actions and reactions. Curr Atheroscler Rep. 2009;11:214-9.

[37] Tanimoto A, Sasaguri Y, Ohtsu H. Histamine network in atherosclerosis. Trends Cardiovasc Med. 2006;16:280-4.

[38] Massberg S, Brand K, Gruner S, Page S, Muller E, Muller I, et al. A critical role of platelet adhesion in the initiation of atherosclerotic lesion formation. J Exp Med. 2002;196:887-96.

[39] Brydon L, Magid K, Steptoe A. Platelets, coronary heart disease, and stress. Brain Behav Immun. 2006;20:113-9.

[40] Fuster V, Badimon J, Chesebro JH, Fallon JT. Plaque rupture, thrombosis, and therapeutic implications. Haemostasis. 1996;26 Suppl 4:269-84.

[41] Huo Y, Ley KF. Role of Platelets in the Development of Atherosclerosis. Trends Cardiovas Med. 2004;14:18-22.

[42] Liu Q, Rooney MM, Kasirer-Friede A, Brown E, Lord ST, Frojmovic MM. Role of the gamma chain Ala-Gly-Asp-Val and Aalpha chain Arg-Gly-Asp-Ser sites of fibrinogen in coaggregation of platelets and fibrinogen-coated beads. Biochim Biophys Acta. 1998;1385:33-42.

[43] Zarbock A, Polanowska-Grabowska RK, Ley K. Platelet-neutrophil-interactions: linking hemostasis and inflammation. Blood Rev. 2007;21:99-111.

[44] Frenette PS, Moyna C, Hartwell DW, Lowe JB, Hynes RO, Wagner DD. Platelet-endothelial interactions in inflamed mesenteric venules. Blood. 1998;91:1318-24.

[45] McEver RP. P-Selectin/PSGL-1 and other interactions between platelets, leukocytes, and endothelium. In: Alan DM, Md, editors. Platelets (Second Edition). Burlington: Academic Press; 2007. p. 231-49.

[46] Reininger AJ, Heijnen HF, Schumann H, Specht HM, Schramm W, Ruggeri ZM. Mechanism of platelet adhesion to von Willebrand factor and microparticle formation under high shear stress. Blood. 2006;107:3537-45.

[47] McCarty OJ, Larson MK, Auger JM, Kalia N, Atkinson BT, Pearce AC, et al. Rac1 is essential for platelet lamellipodia formation and aggregate stability under flow. J Biol Chem. 2005;280:39474-84.

[48] Israels SJ. Platelet function in the newborn. In: Alan DM, Md, editors. Platelets (Second Edition). Burlington: Academic Press; 2007. p. 431-42.

[49] Maintz L, Novak N. Histamine and histamine intolerance. The American Journal of Clinical Nutrition. 2007;85:1185-96.

[50] Jeannin P, Delneste Y, Gosset P, Molet S, Lassalle P, Hamid Q, et al. Histamine induces interleukin-8 secretion by endothelial cells. Blood. 1994;84:2229-33.

[51] Vannier E, Dinarello CA. Histamine enhances interleukin (IL)-1-induced IL-1 gene expression and protein synthesis via H2 receptors in peripheral blood mononuclear cells. Comparison with IL-1 receptor antagonist. J Clin Invest. 1993;92:281-7.

[52] Konstantopoulos K, Kukreti S, Smith CW, McIntire LV. Endothelial P-selectin and VCAM-1 each can function as primary adhesive mechanisms for T cells under conditions of flow. J Leukoc Biol. 1997;61:179-87.

[53] Burns JA, Issekutz TB, Yagita H, Issekutz AC. The alpha 4 beta 1 (very late antigen (VLA)-4, CD49d/CD29) and alpha 5 beta 1 (VLA-5, CD49e/CD29) integrins mediate beta 2 (CD11/CD18) integrin-independent neutrophil recruitment to endotoxin-induced lung inflammation. J Immunol. 2001;166:4644-9.

[54] Labrador V, Riha P, Muller S, Dumas D, Wang X, Stoltz JF. The strength of integrin binding between neutrophils and endothelial cells. Eur Biophys J. 2003;32:684-8.

[55] Budworth RA, Anderson M, Clothier RH, Leach L. Histamine-induced Changes in the Actin Cytoskeleton of the Human Microvascular Endothelial Cell line HMEC-1. Toxicol In Vitro. 1999;13:789-95.

[56] Baldwin AL, Thurston G. Changes in endothelial actin cytoskeleton in venules with time after histamine treatment. Am J Physiol. 1995;269:H1528-37.

[57] Naomasa N, Norio N, Shoso Y. The effect of histamine on cultured endothelial cells A study of the mechanism of increased vascular permeability. Eur J Pharmacol. 1992;221:325-31.

[58] Kitamura Y, Taguchi T, Yokoyama M, Inoue M, Yamatodani A, Asano H, et al. Higher susceptibility of mast-cell-deficient W/WV mutant mice to brain thromboembolism and mortality caused by intravenous injection of India ink. Am J Pathol. 1986;122:469-80.

[59] Valent P, Baghestanian M, Bankl HC, Sillaber C, Sperr WR, Wojta J, et al. New aspects in thrombosis research: possible role of mast cells as profibrinolytic and antithrombotic cells. Thromb Haemost. 2002;87:786-90.

[60] Nemmar A, Hoet PH, Vermylen J, Nemery B, Hoylaerts MF. Pharmacological stabilization of mast cells abrogates late thrombotic events induced by diesel exhaust particles in hamsters. Circulation. 2004;110:1670-7.

[61] Ozben B, Erdogan O. The role of inflammation and allergy in acute coronary syndromes. Inflamm Allergy Drug Targets. 2008;7:136-44.

[62] Bernardo A, Ball C, Nolasco L, Choi H, Moake JL, Dong JF. Platelets adhered to endothelial cell-bound ultra-large von Willebrand factor strings support leukocyte tethering and rolling under high shear stress. J Thromb Haemost. 2005;3:562-70.

[63] Chen C, Khismatullin DB. Synergistic effect of histamine and TNF-α on monocyte adhesion to vascular endothelial cells. Inflammation. (2012, in press).